Electrical characterisation of the insulating property of Ta_2O_5 in Al–Ta_2O_5–SiO_2–Si capacitors by a low-frequency C/V technique

J.-G. Hwu
S.-T. Lin

Indexing terms: Metal–oxide–semiconductor structures

Abstract: The measurement of equivalent low-frequency capacitance is used as an efficient method to monitor the insulating properties of Ta_2O_5 in Al–Ta_2O_5–SiO_2–Si (MTOS) structures. It is found however, that MTOS devices having normal high-frequency C/V characteristics can have significantly different behaviour at low frequencies. A technique is proposed in this work that enables the quality of the Ta_2O_5 preparation to be determined. Examples showing the importance of the measurement of the equivalent low-frequency capacitance are also given.

1 Introduction

Tantalum oxide (Ta_2O_5) is useful as a capacitor material in some memory applications because of its high dielectric constant (20–25) [1]. Generally, it can be prepared by direct sputtering [2–4], thermal oxidation of evaporated Ta [5–7], anodisation [8] or chemical vapour deposition [9]. Since the insulating property of Ta_2O_5 is the most important parameter in Ta_2O_5-based devices, almost all workers have examined Ta_2O_5 films by measuring the I/V curve [1, 4, 7] or the high-frequency C/V [2, 3, 5, 6] characteristics of their devices. It is interesting to note that although the conventional quasistatic C/V technique is essential in examining the interface property between an insulating layer and the Si substrate [10], it has not been successfully applied to any Ta_2O_5-based device in the literature. This is mainly because the conduction current of Ta_2O_5 is comparable to the displacement current for most gate voltages [7].

In this work, we analyse the quasistatic C/V curves of Al–Ta_2O_5–SiO_2–Si (MTOS) capacitors because they can show much information about the insulating property of Ta_2O_5. Note that the low-frequency capacitance obtained by the quasistatic C/V technique is an equivalent capacitance, i.e. $C_{LF(eq)}$, because it contains both the displacement and conduction currents. The effect of the conduction current in Ta_2O_5 on the $C_{LF(eq)}$ of MTOS structures is basically different from the effect of leakage current observed in MOS structures [11]. A qualitative explanation of this is given below.

Both sputtered and thermal Ta_2O_5 are investigated. The prepared MTOS capacitors all show quite good high-frequency C/V curves from which one can determine the quantities of the effective fixed charges. However, when the low-frequency C/V characteristics are examined for these samples, one can clearly observe differences in $C_{LF(eq)}$ between them. Since $C_{LF(eq)}$ is sensitive to the insulating property of Ta_2O_5 one can deduce the quality of the Ta_2O_5 from a comparison between $C_{LF(eq)}$ and the high-frequency capacitance C_{HF}.

From the experimental observations, it is found that, when a sputtered Ta_2O_5 device receives a postmetallisation anneal at 300°C in N_2, the insulating property of Ta_2O_5 becomes poor, although the positive fixed charge is significantly reduced. Interestingly, it is also observed that, for a thermal Ta_2O_5 device, the H_2 anneal at 450°C reduces the number of interface trap states significantly, but does not give any improvement in the insulating property of Ta_2O_5, i.e. the Ta_2O_5 becomes leaky after H_2 annealing. The reduction of the numbering interface trap states after H_2 annealing is consistent with that observed by Seki in sputtered Ta_2O_5 films, based on the high-frequency C/V technique [3]. However, the change in the insulating property of Ta_2O_5 as a result of the H_2 anneal, as observed in this work, is also important in the study. In addition, since the oxidation condition is important to thermal Ta_2O_5, the dependence of $C_{LF(eq)}$ on oxidation time is also examined. It is found that $C_{LF(eq)}$ is indeed sensitive to the oxidation time and an optimal oxidation time can therefore be determined from the observed $C_{LF(eq)}$ behaviour. Finally, we use the recently reported radiation-then-anneal method [12] to improve the performance of MTOS devices. Briefly, when an MOS capacitor receives repeated radiation-then-anneal treatments, its radiation resistance is much improved. In this work, we find that the fixed charges, the interface trap states and the insulating property of Ta_2O_5 are all improved by this method. A possible explanation is also given.

2 Experiment

p-type and n-type silicon wafers with (100)-orientation were used as the substrates of MTOS capacitors. After standard cleaning procedures, these wafers were dry-oxidised at 900°C to various oxide thicknesses. Then, two kinds of Ta_2O_5 film were formed on SiO_2/Si. One is reactively sputtered Ta_2O_5, obtained under a partial pressure ratio of $Ar/O_2 = 4/1$, the other is thermal Ta_2O_5, made by oxidation of an electron-beam-deposited Ta film under O_2/N_2 at a flow rate ratio of 6/5 at 540°C. Further, aluminum was thermally evaporated on to the samples through metal masks to form contact electrodes. The area of the device discussed in this work was defined by

Paper 7473G (E3), first received 2nd October 1989 and in revised form 21st February 1990

The authors are with the Department of Electrical Engineering, National Taiwan University, Taipei, Taiwan, Republic of China

the area of the aluminum contact electrode. On the backside of the samples, aluminum was also evaporated, after the oxide was etched away. Note that the thicknesses of Ta_2O_5 were measured by ellipsometry. The surface topography and the thickness uniformity of Ta_2O_5 are not discussed in this work.

Fig. 1*a* shows the high-frequency (1 MHz) capacitance C_{HF} plotted against the gate voltage V_G of three MTOS

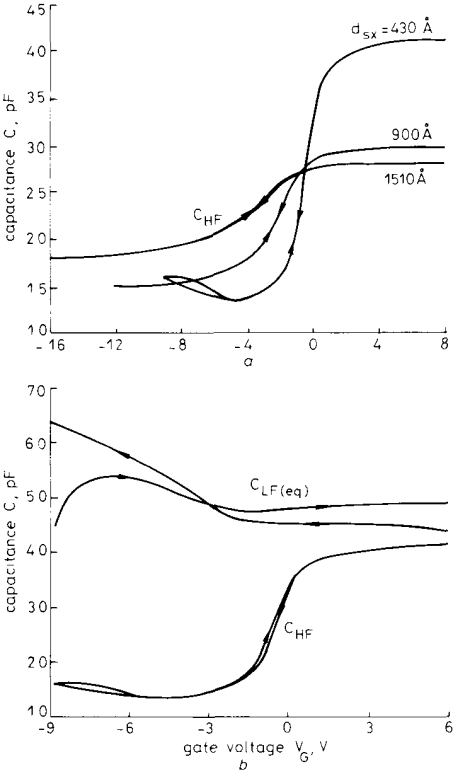

Fig. 1 *Change in capacitance characteristics caused by change in dV_G/dt for MTOS (n) capacitors*

a High-frequency capacitance C_{HF} against gate voltage V_G curves of three capacitors with silicon oxide thicknesses d_{sx} of 430 (SN-1), 900 (SN-2) and 1510 (SN-3) Å and a common tantalum oxide thickness d_{tx} of 350 Å. The Ta_2O_5 is prepared by direct sputtering

b C_{HF} and equivalent low-frequency capacitance $C_{LF(eq)}$ against V_G curves of a capacitor with a d_{tx} of 350 Å and a d_{sx} of 430 Å (SN-1)
$|dV_G/dt| = 0.02$ V/s
Hold time = 10 s

(*n*) capacitors, measured using an HP 4275A. The Ta_2O_5, having a tantalum oxide thickness d_{tx} of 350 Å, was prepared by direct sputtering. The thicknesses of silicon oxides d_{sx} for samples SN-1, SN-2 and SN-3, were 430, 900, and 1510 Å, respectively. Note that none of these samples received a postmetallisation anneal. The capacitors seem quite good for these C_{HF} curves because their hysteresis loops are insignificant and are clockwise in direction. The clockwise hysteresis phenomenon for MTOS (*n*) capacitors is mainly the result of the trapping of holes at the SiO_2/Si interface, but not the leakage current through Ta_2O_5 [5]. Therefore, not much information about the insulating property of Ta_2O_5 can be determined from these curves. However, when the conventional quasistatic C/V technique is performed on the sample SN-1 using an HP 4140B with a sweep rate $|dV_G/dt|$ of 0.02 V/s and a hold time of ten seconds, abnormal capacitance behaviour appears. As can be seen from the C/V curves in Fig. 1*b*, $C_{LF(eq)}$ is larger than C_{HF} for almost the whole range of V_G and there is a split between the curves obtained under forward and backward sweeps.

Similarly, an MTOS (*p*) capacitor prepared under the same conditions as mentioned in Fig. 1 was also examined. Fig. 2*a* shows the C/V curves of an MTOS (*p*) capacitor, i.e. SP-1, with a d_{tx} of 266 Å and a d_{sx} of 270 Å. It is clear that the $C_{LF(eq)}$ behaviour is independent of the substrate type. However, when the sweep rate varies, the $C_{LF(eq)}$ behaviour changes, as can be seen from Fig. 2*b*, the splitting between the $C_{LF(eq)}$ curves obtained under forward and backward sweeps decreases as the sweep rate increases.

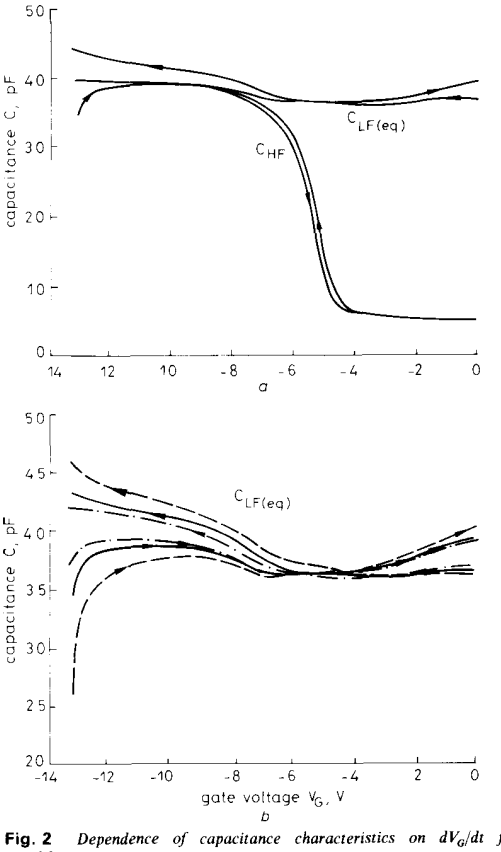

Fig. 2 *Dependence of capacitance characteristics on dV_G/dt for MTOS (p) capacitor*

a C_{HF} and $C_{LF(eq)}$ against V_G curves of a capacitor with a d_{tx} of 266 Å and a d_{sx} of 270 Å (SP-1). The Ta_2O_5 is prepared by direct sputtering
$|dV_G/dt| = 0.02$ V/s
Hold time = 10 s

b Sweep rate dependence of $C_{LF(eq)}$ curves for the same sample
- - - - $|dV_G/dt| = 0.01$ V/s
——— $|dV_G/dt| = 0.02$ V/s
—·—· $|dV_G/dt| = 0.04$ V/s

3 Discussion and examples

3.1 Equivalent low-frequency C/V behaviour

Generally, the $C_{LF(eq)}$ obtained by the quasistatic C/V technique is obtained by dividing the measured current I

by dV_G/dt. The measured current is purely the displacement current I_D for an ideal capacitor, but may consist of conduction current I_R when the sample is leaky [11]. In this work, there are two layers, i.e. Ta_2O_5 and SiO_2, in an MTOS capacitor. The SiO_2 layer can be regarded as an ideal insulator with respect to the Ta_2O_5 layer. The charges moving within the Ta_2O_5 layer due to the electric field introduce an I_R component to the total measured I and are accumulated somewhere in the Ta_2O_5. Since the growth of pinholes is unstable, the conduction mechanism within the Ta_2O_5 is complicated [4, 13], and is basically different from that for the leakage current that flows through a device similar to an MOS capacitor [11]. Fig. 3 shows the simplified equivalent circuit of an

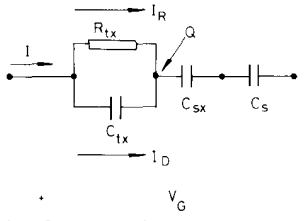

Fig. 3 *Simplified equivalent circuit for an MTOS capacitor with a Ta_2O_5 leakage resistance R_{tx}*

C_{tx}, C_{sx} and C_s are the capacitances of Ta_2O_5, SiO_2 and Si, respectively. I_R and I_D are the conduction current and the displacement current through Ta_2O_5, respectively, during low-frequency C/V measurement. Q is the effective trapped charge within the Ta_2O_5. I is the total measured current

$$C_{LF(eq)} = \frac{I_R + I_D}{dV_G/dt}$$

$$I = I_R + I_D$$

MTOS capacitor. C_{tx}, C_{sx}, and C_s are the capacitances of Ta_2O_5, SiO_2 and silicon substrate, respectively. R_{tx} represents the leakage resistance of Ta_2O_5, which is a complicated function of V_G, dV_G/dt and the charges trapped in the Ta_2O_5 layer Q. When I_R is important, I can be written as

$$I = I_D + I_R \tag{1}$$

Then, $C_{LF(eq)}$ can be expressed as

$$C_{LF(eq)} = \frac{I_R + I_D}{\frac{dV_G}{dt}} \tag{2}$$

When V_G sweeps from negative to positive, i.e. $dV_G/dt > 0$, I_D is positive over the whole V_G range, but I_R may change from negative to positive during a sweep. Therefore, the contribution of I_R to $C_{LF(eq)}$ is first subtracted, when the directions of I_R and I_D are opposite, and is then added when the directions are the same. Similarly, when V_G sweeps from positive to negative, i.e. $dV_G/dt < 0$, the same effect on the contribution of I_R to $C_{LF(eq)}$ occurs as is described above. Near the positive V_G range, I_D is negative, but I_R is positive so $C_{LF(eq)}$ is reduced. While near the negative V_G range, I_D and I_R are both negative so $C_{LF(eq)}$ is increased. It is clear from the above discussion that I_R accounts for the splitting of the $C_{LF(eq)}$ curves, and the dependency of $C_{LF(eq)}$ on dV_G/dt, as observed in Fig. 2*b*, is explainable.

It is also noted that the condition when I_R changes sign during forward or backward sweeping depends on the electric field that the Ta_2O_5 layer has sustained. When the trapped negative charge in the Ta_2O_5 is large, it is possible that the electric field in the Ta_2O_5 is still positive at a certain negative V_G during forward sweeping. Under such a circumstance, I_R and I_D are both positive and contribute a higher value of $C_{LF(eq)}$ than C_{HF} over the whole V_G range. Similarly, the same behaviour can also occur during backward sweeping. Therefore, the higher value of $C_{LF(eq)}$ compared with C_{HF} observed in MTOS capacitors is basically different from that observed in an MOS capacitor. However, it is sufficient to note that the measurement of $C_{LF(eq)}$ can be a useful method by which to examine the insulating property of Ta_2O_5 in MTOS structures.

3.2 Effects of postmetallisation annealing in N_2

Generally, when an MTOS device receives a postmetallisation annealing, its interface trap states and fixed oxide charges can be reduced to an insignificant level. However, there is lack of information about the effect of postmetallisation annealing on the insulating property of Ta_2O_5. Fig. 4 shows the C_{HF} and $C_{LF(eq)}$ curves of the MTOS (*p*)

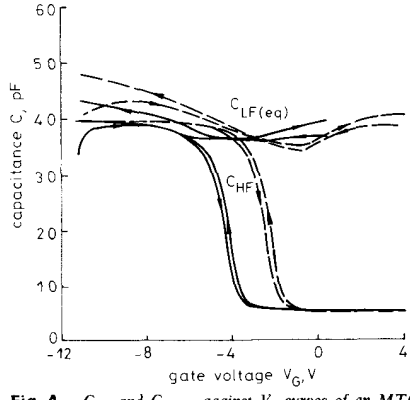

Fig. 4 *C_{HF} and $C_{LF(eq)}$ against V_G curves of an MTOS (p) capacitor (SP-1) before and after postmetallisation annealing in N_2 at 300°C for ten minutes*

The Ta_2O_5 is prepared by direct sputtering
d_{tx} = 266 Å
d_{sx} = 270 Å
——— before annealing
- - - - after annealing

capacitor with sputtered Ta_2O_5 as discussed in relation to Fig. 2, i.e. SP-1, before and after receiving a postmetallisation annealing in N_2 at 300°C for 10 minutes. It is clear that the insulating property of Ta_2O_5 becomes poor after annealing since $C_{LF(eq)}$ after annealing is larger than that before annealing. The shift of C_{HF} as a result of annealing accounts for the reduction of the effective positive oxide fixed charge. Unfortunately, this anneal is insufficient to eliminate the slow trapping states since the counterclockwise hysteresis loop is still distinguishable after annealing. So, it can be noted from the above discussion that the measurement of $C_{LF(eq)}$, in addition to C_{HF}, is important when analysing an MTOS device after it has been subjected to a thermal annealing. It is noted that the possible chemical reaction during annealing, between the aluminium metal electrode and the Ta_2O_5, is beyond discussion in this work. However, since the maximum values of C_{HF} before and after annealing are almost equal, the change in the effective area due to this reaction is negligible.

3.3 Effects of postoxidation annealing in H_2

To show the effect of postoxidation annealing in H_2 on the insulating property of Ta_2O_5, two MTOS (*p*) capacitors, i.e. TP-1 and TP-2, were compared. The Ta_2O_5

layers in these samples were prepared by thermal oxidation at 540°C for 90 minutes simultaneously. The final thicknesses of Ta_2O_5 and SiO_2 layers were 650 Å and 400 Å, respectively. It should be noted that TP-2 received a postoxidation annealing in H_2 at 450°C for 30 minutes, but TP-1 did not. Their normalised C/V curves are shown in Fig. 5. Note that the behaviour of $C_{LF(eq)}$ for

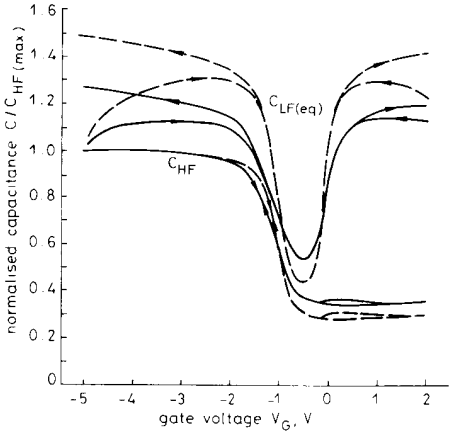

Fig. 5 *Normalised C_{HF} and $C_{LF(eq)}$ against V_G curves of two MTOS (p) capacitors with (TP-2) and without (TP-1) postoxidation annealing in H_2 at 450°C for 30 minutes*

The Ta_2O_5 is prepared by thermal oxidation at 540°C for 90 minutes
d_{ix} = 650 Å
d_{sx} = 400 Å
——— no H_2 annealing
- - - - H_2 annealed

thermally grown Ta_2O_5, as shown in Fig. 5, is different from that for sputtered Ta_2O_5, as shown in Fig. 4. This is mainly due to the radiation damage to the Ta_2O_5 during sputtering. As can be seen from the C_{HF} curves, TP-2 appears to exhibit a steeper behaviour with respect to changing gate voltage than TP-1 in the depletion region and there is no hysteresis phenomenon for either sample. Therefore, the number of slow trap states is negligible and the number of interface trap states can be significantly reduced by H_2 annealing. However, as can be seen from the $C_{LF(eq)}$ curves, TP-2 appears to have a larger value for and a larger split in $C_{LF(eq)}$ than TP-1 so the insulating property of Ta_2O_5 becomes poor after H_2 annealing. It seems quite clear from Figs. 4 and 5 that this property of Ta_2O_5 is very sensitive to a thermal treatment.

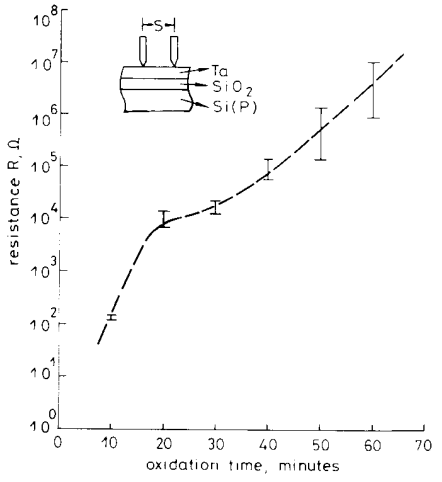

Fig. 6 *Resistance R against oxidation time of an MTOS (p) capacitor (TP-3) oxidised at 540°C*

The space S between the two measurement probes is 2 mm

3.4 Optimal oxidation time for thermal Ta_2O_5

For thermal oxidation of a Ta film at a certain temperature, the oxidation time is one of the important parameters. However, it is rather difficult to accurately control the oxidation time, since it depends on the thickness of Ta film and the oxidation conditions. In this work, we propose that the insulating property of Ta_2O_5 during thermal oxidation be detected by measuring and plotting surface resistance R and current I against V_G or $C_{LF(eq)}$ against V_G.

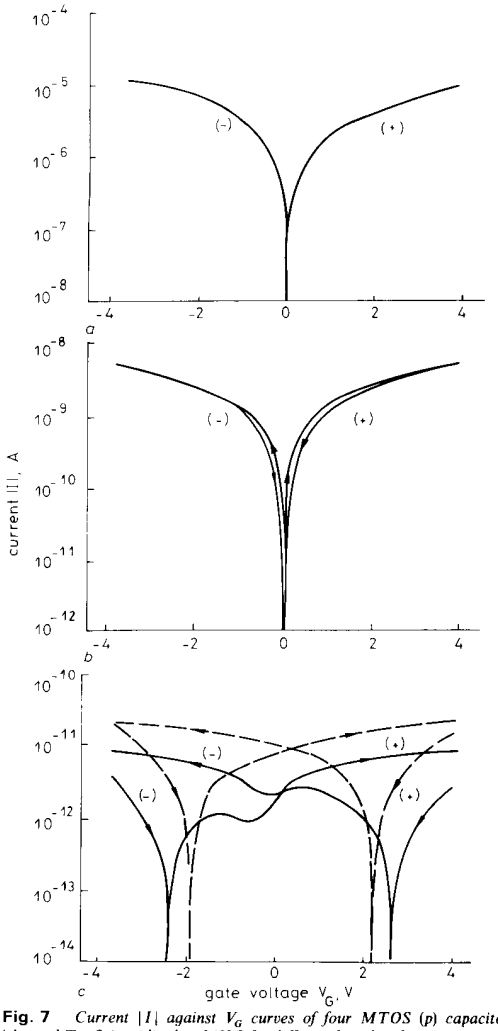

Fig. 7 *Current $|I|$ against V_G curves of four MTOS (p) capacitors (thermal Ta_2O_5) oxidised at 540°C for different lengths of time*

d_{sx} = 400 Å; $|dV_G/dt|$ = 0.02 V/s
a 60 minutes (TP-4-1)
b 70 minutes (TP-4-2)
c 90 and 110 minutes
- - - - 90 minutes (TP-4-3)
——— 110 minutes (TP-4-4)

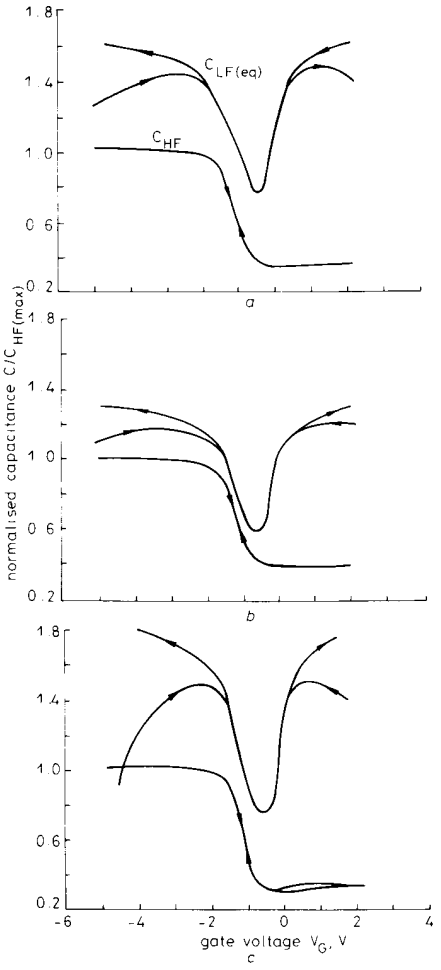

Fig. 8 *Normalised C_{HF} and $C_{LF(eq)}$ against V_G curves of three MTOS (p) capacitors (thermal Ta_2O_5) oxidised at 540°C for different lengths of time*

d_{ix} = 650 Å; d_{ax} = 400 Å; $|dV_G/dt|$ = 0.02 V/s
a 75 minutes (TP-5-1)
b 90 minutes (TP-5-2)
c 105 minutes (TP-5-3)

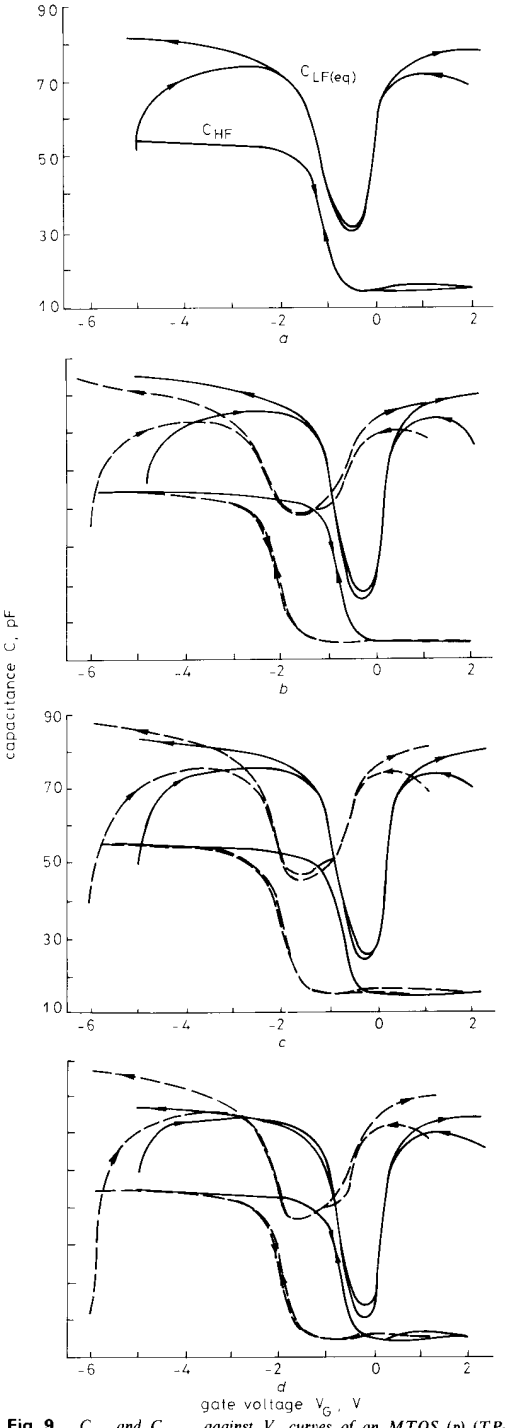

Fig. 9 *C_{HF} and $C_{LF(eq)}$ against V_G curves of an MTOS (p) (TP-6) capacitor (thermal Ta_2O_5)*

a After postmetallisation annealing (400°C, N, 10 min)
b After first radiation and anneal treatment
c After second treatment
d After third treatment
d_{ax} = 360 Å — — — irradiated (Co^{60}, 10 kGy)
d_{ix} = 500 Å —·—·— annealed

In the early period of thermal oxidation, most of the Ta film is still conductive so the surface resistance of the sample under test can be easily measured using a multimeter. Fig. 6 shows R against oxidation time for a sample, i.e., TP-3, oxidised at 540°C. The thickness of the SiO_2 layer under the Ta film is 400 Å. The space between the two measurement probes S is 2 mm. Note that the probes touch the sample surface directly without preparation of the contact electrode. As expected, the resistance increases as the oxidation time increases. When the oxidation time exceeds about 1 h, R is too high to be accurately measured in this way.

If the $C_{LF(eq)}$ technique mentioned above is used in a very leaky sample, the capacitance value is beyond the range of the HP 4140B meter, because of the large current. It is therefore better to make measurements in the current mode rather than the capacitance mode under such a circumstance. Fig. 7 shows the absolute

current $|I|$ against V_G for four samples, i.e., TP-4-1, TP-4-2, TP-4-3 and TP-4-4, oxidised at 540°C for 60, 70, 90 and 110 minutes, respectively. The sweep rate is $|dV_G/dt| = 0.02$ V/s for each measurement. As can be seen from Fig. 7*a*, the current is quite large. This is mainly due to the conduction current through the Ta_2O_5. Sample TP-4-1 is very conductive, but for sample TP-4-2, as shown in Fig. 7*b*, the displacement current of the Ta_2O_5 is no longer negligible because the conduction current of the Ta_2O_5 decreases. This contributes a small hysteresis phenomenon to the $|I|$ against V_G curves shown in this figure. When the oxidation time increases to 90 or 110 minutes, as shown in Fig. 7*c*, the conduction current of Ta_2O_5 decreases further and the displacement current becomes a greater proportion of $|I|$. However, the oxidation time of 90 or 110 minutes is still not good enough since the hysteresis phenomena for samples TP-4-3 and TP-4-4 are both significant.

Figs. 8*a*, *b* and *c* show the normalised capacitance $C/C_{HF(max)}$ against V_G for three other samples, i.e. TP-5-1, TP-5-2 and TP-5-3, oxidised at 540°C for 75, 90 and 105 minutes, respectively. Note that the initial thickness of the Ta films for these samples are different from those of the films whose characteristics are shown in Fig. 7 and that the optimal oxidation time for the samples of Fig. 8 is different from that for those in Fig. 7. As can be seen from Fig. 8, all the C_{HF} curves are good enough to be distinguished. But, an oxidation time of 90 minutes gives the best $C_{LF(eq)}$ behaviour of the three. A long oxidation time may enhance the growth of pinholes and therefore increase the leakage current [4].

3.5 *Improvement of the insulating property of Ta_2O_5 by repeated radiation-then-anneal treatments*

When an MTOS capacitor receives Co^{60} irradiation to a total dose of 10 kGy, the radiation-induced holes (or electrons) can be partially trapped in the oxide layers by the hole (or electron) trapping centres. Therefore, the C/V curve after irradiation will shift, because of the change in the effective trapped charge. However, when the irradiated MTOS capacitor receives a subsequent anneal in N_2 at 400°C for ten minutes, the radiation-induced damage can be substantially eliminated. Fig. 9 shows the C/V curves for a thermal MTOS capacitor, i.e. TP-6, before and after such treatments. Fig. 9*a* shows the C/V curves after postmetallisation annealing (PMA). The C/V curves after the first, second and third radiation and anneal treatments are shown in Figs. 9*b*, *c* and *d*, respectively. There are some important phenomena to observe in these figures. For a clear understanding, the C/V curves after PMA, i.e. the curves in Fig. 9*a*, and after repeated radiation-then-anneal treatments, i.e. the solid curves in Fig. 9*d*, are shown together in Fig. 10. From the C_{HF} curves, it is to be noted that the numbers of effective positive charges in the insulators are significantly reduced after treatments. Furthermore, from the comparisons between the $C_{LF(eq)}$ curves and the C_{HF} curves near the depletion region, the number of interface trap states at the SiO_2/Si interface is also reduced. Interestingly, the splitting of the $C_{LF(eq)}$ curves after treatment is smaller than that before treatment. Therefore, the insulating property of Ta_2O_5 is improved by this method. This is probabily because of the removal of the strain, related to trapping centres in the Ta_2O_5, which are responsible for its conduction current, by repeated radiation-then-anneal treatments [14].

Finally, the flat-band voltage V_{FB} and the effective fixed charge Q_{eff} against the number of treatments are shown in Fig. 11, based on the C/V curves shown in Fig. 9. It is clear that V_{FB} (or Q_{eff}) decreases gradually after each radiation or each anneal as the number of treat-

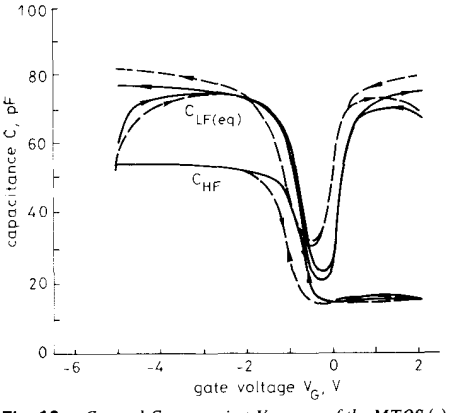

Fig. 10 *C_{HF} and $C_{LF(eq)}$ against V_G curves of the MTOS (p) capacitor of Fig. 9 before and after repeated radiation-then-anneal treatments*

- - - postmetallisation annealed (400°C, N_2, 10 min)
——— repeatedly radiation-then-anneal treated

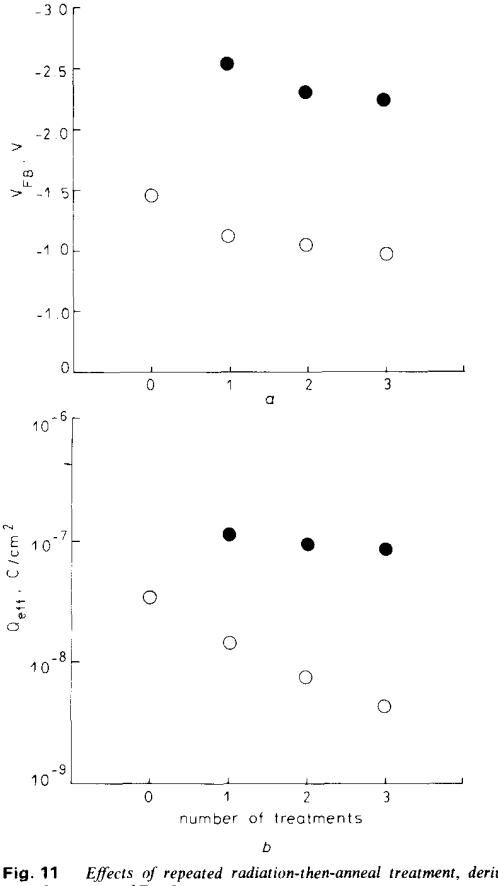

Fig. 11 *Effects of repeated radiation-then-anneal treatment, derived from C_{HF} curves of Fig. 9*

a Effect on flat-band voltage V_{FB}
b Effect on effective fixed charge Q_{eff}
● after radiation (Co^{60}, 10 kGy)
○ after anneal (400°C, N_2, 10 min)

ments increases. Therefore, the 'radiation-hardness' of MTOS capacitors is also improved by this method.

4 Conclusions

Observation of the equivalent low-frequency capacitance of an MTOS capacitor gives one a method of direct examination of the insulating property of Ta_2O_5. By the use of this technique, a dependence on the process of preparation of the Ta_2O_5 is found. The insulating property of Ta_2O_5 becomes poor when it receives a post metallisation anneal in N_2 or a postoxidation anneal in H_2. For thermal Ta_2O_5, the optimal oxidation time is achievable by examination of the condition when the $C_{LF(eq)}$ behaviour is least leaky. Repeated radiation-then-anneal treatments improve the insulating property of Ta_2O_5 and also reduce the effective positive fixed charge and the concentration of interface trap stages.

5 Acknowledgment

The authors want to thank the National Science Council of the Republic of China for the support of this work under contract No. NSC78-0404-E002-01.

6 References

1 OHTA, K., YAMADA, K., SHIMIZU, K., and TARUI, Y.: 'Quadruply self-aligned stacked high-capacitance RAM using Ta_2O_5 high-density VLSI dynamic memory', *IEEE Trans.*, 1982, **ED-29**, pp. 368–376

2 ROBERT, S., RYAN, J., and NESBIT, L.: 'Selective studies of crystalline Ta_2O_5 films', *J. Electrochem. Soc.*, 1986, **133**, pp. 1405–1410

3 SEKI, S., UNAGAMI, T., and TSUJIYAMA, B.: 'Electrical characteristics of tantalum pentoxide–silicon dioxide–silicon structures', *ibid.*, 1985, **132**, pp. 199–202

4 KIMURA, S., NISHIOKA, Y., SHINTANI, A., and MUKAI, K.: 'Leakage-current increase in amorphous Ta_2O_5 films due to pinhole growth during annealing below 600°C', *ibid.*, 1983, **130**, pp. 2414–2418

5 HWU, J.G., JENG, M.J., WANG, W.S., and TU, Y.K.: 'Clockwise C–V hysteresis phenomena of metal–tantalum oxide–silicon oxide–silicon (p) capacitors due to leakage current through tantalum oxide', *J. Appl. Phys.*, 1987, **62**, pp. 4277–4283

6 HWU, J.G., and JENG, M.J.: 'C–V hysteresis instability in aluminum/tantalum oxide/silicon oxide/silicon capacitors due to postmetallization annealing and Co-60 irradiation', *J. Electrochem. Soc.*, 1988, **135**, pp. 2808–2813

7 OEHRLEIN, G.S.: 'Capacitance-voltage properties of thin Ta_2O_5 films on silicon', *Thin Solid Films*, 1988, **156**, pp. 207–229

8 ANGLE, R.L., and TALLEY, H.E.: 'Electrical and charge storage characteristics of the tantalum oxide–silicon dioxide device', *IEEE Trans.*, 1978, **ED-25**, pp. 1277–1283

9 KAPLAN, E., BALOG, M., and BENTCHKOWSKY, D.F.: 'Chemical vapor deposition of tantalum pentoxide films for metal–insulator–semiconductor devices', *J. Electrochem. Soc.*, 1976, **123**, pp. 1570–1573

10 MANCHANDA, L., and GURVITCH, M.: 'Yttrium oxide/silicon dioxide: a new dielectric structure for VLSI/ULSI circuits', *IEEE Electron Device Lett.*, 1988, **9**, pp. 180–182

11 MONDERER, B., and LAKHANI, A.A.: 'Measurement of the quasi-static C–V curves of an MIS structure in the presence of charge leakage', *Solid-State Electron.*, 1985, **28**, pp. 447–451

12 HWU, J.G., and FU, S.L.: 'Improvement in radiation hardness of oxide by successive irradiation-then-anneal treatments', *ibid.*, 1989, **32**, pp. 615–620

13 OEHRLEIN, G.S.: 'Oxidation temperature dependence of the dc electrical conduction characteristics and dielectric strength of thin Ta_2O_5 films on silicon', *J. Appl. Phys.*, 1986, **59**, pp. 1587–1595

14 HWU, J.G., and CHEN, J.T.: 'Improvement of hot-electron-induced degradation in MOS capacitors by repeated irradiation-then-anneal treatments', *IEEE Electron Device Lett.*, 1990, **11**, pp. 82–84